



## Article

# Remaining Useful Life Prediction for Lithium-Ion Batteries Based on Improved Variational Mode Decomposition and Machine Learning Algorithm

Chuang Sun <sup>1</sup> , An Qu <sup>2</sup>, Jun Zhang <sup>1</sup>, Qiyang Shi <sup>1</sup>  and Zhenhong Jia <sup>1,\*</sup><sup>1</sup> College of Information Science and Engineering, Xinjiang University, Urumqi 830046, China<sup>2</sup> Network Management Center, China Mobile Xinjiang Co., Ltd., Urumqi 830063, China

\* Correspondence: jzh@xju.edu.cn

**Abstract:** Remaining useful life (RUL) prediction of batteries is important for the health management and safety evaluation of lithium-ion batteries. Because lithium-ion batteries have capacity recovery and noise interference during actual use, direct use of measured capacity data to predict their RUL generalization ability is not efficient. Aimed at the above problems, this paper proposes an integrated life prediction method for lithium-ion batteries by combining improved variational mode decomposition (VMD) with a long short-term memory network (LSTM) and Gaussian process regression algorithm (GPR). First, the VMD algorithm decomposed the measured capacity dataset of the lithium-ion battery into a residual component and capacity regeneration component, in which the penalty factor  $\alpha$  and mode number  $K$  in the VMD algorithm were optimized by the whale optimization algorithm (WOA). Second, the LSTM and GPR models were established to predict the residual component and capacity regeneration components, respectively. Last, the predicted components are integrated to obtain the final predicted lithium-ion battery capacity. The experimental results show that the mean absolute error (MAE) and root mean square error (RMSE) of the proposed lithium-ion battery capacity prediction model are less than 0.5% and 0.8%, respectively, and the method outperforms the five compared algorithms and several recently proposed hybrid algorithms in terms of prediction accuracy.

**Keywords:** lithium-ion battery; variational mode decomposition; remaining useful life prediction; long short-term memory; Gaussian process regression



**Citation:** Sun, C.; Qu, A.; Zhang, J.; Shi, Q.; Jia, Z. Remaining Useful Life Prediction for Lithium-Ion Batteries Based on Improved Variational Mode Decomposition and Machine Learning Algorithm. *Energies* **2023**, *16*, 313. <https://doi.org/10.3390/en16010313>

Academic Editors: Desmond Gibson, Mojtaba Mirzaei, Peter Hall and Saule Aidarova

Received: 23 November 2022

Revised: 25 December 2022

Accepted: 25 December 2022

Published: 27 December 2022



**Copyright:** © 2022 by the authors. Licensee MDPI, Basel, Switzerland. This article is an open access article distributed under the terms and conditions of the Creative Commons Attribution (CC BY) license (<https://creativecommons.org/licenses/by/4.0/>).

## 1. Introduction

With the development of battery technology, lithium-ion batteries (LIBs) have become the most frequently employed battery type because of their high density, light weight, cleanliness, environmental friendliness, and excellent electrochemical performance. LIBs are widely employed in electric vehicles, logistics, aerospace, and military fields [1,2]. Since the existing lithium-ion battery will work at high and low temperatures, this will cause a significant reduction in battery charging efficiency and life, especially in the field of electric vehicles. If the battery health status is not monitored in a timely manner, the battery is likely to thermal runaway, resulting in serious losses [3,4].

Lithium-ion batteries play various important roles in life, and the health status management and RUL prediction of lithium-ion batteries are getting more and more attention. The battery management technology is changing from passive safety protection to active risk prediction [5]. Model-based and data-driven methods are now commonly used for lithium-ion battery RUL forecasting [6].

The model-based prediction methods mainly analyze the electrochemical characteristics of lithium batteries, establish a mathematical or physical degradation model, and predict battery degradation through the model. Shimamoto et al. [7] proposed a method to evaluate the remaining useful life of a battery based on experiments and a degradation

database of lithium-ion battery usage patterns. However, this method has difficulty accurately analyzing the degradation state of the battery. He et al. [8] established an empirical model for the physical degradation behavior of lithium-ion batteries. The parameters of the model were initialized by Dempster–Shafer (DS) theory, and the parameters of the model were updated by Bayesian Monte Carlo (BMC). The RUL of the battery was predicted by the available data in the monitoring data of the battery capacity. Presently, battery RUL prediction combined with a filtering algorithm is a commonly employed technology based on model prediction methods, such as the Kalman filter (KF) and the particle filter (PF). Zhang et al. [9,10] proposed a method based on the extended Kalman filter (EKF) to predict the RUL of lithium-ion batteries. Xiong et al. [11] proposed a double-scale particle filter method to predict the state and parameters of the battery on two different time scales to observe the state of the battery. Park et al. [12] combined anomaly detection technology with the PF algorithm to adaptively predict the RUL according to the state changes during battery degradation. However, the previously described model-based prediction methods have two significant drawbacks: ① Due to its complex electrochemical characteristics, the lithium-ion battery is vulnerable to being disturbed by external environmental factors such as temperature and humidity; therefore, it is complicated to establish an accurate mathematical or physical model, and many parameters are needed [13,14]. ② Particle filtering has obvious particle degradation problems, which can affect the accuracy of the prediction experiment.

Compared with the model-based RUL prediction methods for lithium-ion batteries, the data-driven methods do not rely on establishing a physical or chemical model to predict battery capacity decline. Instead, the data-driven methods extract voltage, temperature, current, and other data from the charging–discharging of lithium-ion batteries and analyze the relationship between these data and the capacity decline, and they realize the RUL prediction of lithium-ion batteries through intelligent algorithms. Commonly employed data-driven methods include the support vector machine (SVM) [15], artificial neural network (ANN) [16], correlation vector machine (RVM) [17,18], and recurrent neural network (RNN) [19]. Yang [20] designed a hybrid convolutional neural network (CNN) to predict the RUL of the battery through the voltage, current, and temperature curves during the charging cycle of lithium-ion batteries. Wei et al. [21] proposed an indirect health indicator combined with Monte Carlo dropout (MC\_dropout) and gated recurrent units (GRUs) to model and predict battery RUL. Due to the different degradation trends of lithium-ion batteries at different stages, it is difficult to establish an accurate battery RUL model [22]. Zhang et al. [23] proposed an extreme learning machine (CTC-ELM)-based prediction model for predicting the RUL of a battery under small sample conditions. Gaussian process regression (GPR) models can be used to solve problems with large dimensions, small amounts of data, and nonlinear regression [24]. Richardson et al. [25] proposed a method for predicting battery remaining useful life based on a Gaussian process. Yu [26] proposed a new prediction method combining multi-scale logical regression (LR) and a GPR model to predict the decline of battery capacity.

Although the above methods can predict the RUL of lithium-ion batteries, the complex degradation trend of lithium-ion batteries will still have the problem of poor prediction accuracy if a single-scale intelligent algorithm is used to predict it. Tong et al. [27] integrated the characteristics of an adaptive dropout long short-term memory network (ADLSTM) and a Monte Carlo (MC) simulation algorithm to enable prediction of the state of health of lithium-ion batteries. Ren et al. [28] proposed a model combining an improved convolutional neural network (CNN) and LSTM algorithm, which uses a CNN to mine deep information and LSTM to obtain time series to predict the remaining useful life of a battery. The above hybrid data-driven method captures the degradation trend of the battery and improves the accuracy of prediction to a certain extent. But they all use the capacity sequence of lithium-ion batteries to predict directly.

The capacity of the original battery sequence fluctuates greatly and contains much noise, so it is difficult to predict it directly [29]. To solve this problem and improve the

prediction accuracy, Cheng et al. [30] selected the empirical mode decomposition (EMD) method to decompose the measured lithium-ion battery capacity series into signals of different frequencies. After removing the capacity regeneration components representing the lithium-ion battery, the bidirectional LSTM predicts the battery life by predicting the residual component. However, the EMD has limitations and is prone to modal confusion, affecting the prediction accuracy. The VMD algorithm is an adaptive signal decomposition technique. Compared with the EMD, this algorithm overcomes the shortcomings of modal aliasing in the EMD algorithm and is more robust to sampling and noise [31].

To effectively capture the phenomenon of the steep rise and fall of battery capacity and solve the problem of insufficient accuracy in prediction, we proposed a hybrid model for the RUL prediction of lithium-ion batteries based on a combination of improved VMD, LSTM, and GPR algorithms. The major contributions are presented as follows:

- (1) A new method for predicting the RUL of lithium-ion batteries is proposed. First, the measured battery capacity sequence is decomposed by the VMD algorithm, and the capacity data are decomposed into residual components and capacity regeneration components. Second, the residual component is predicted by the LSTM algorithm, and the capacity regeneration component is predicted by the GPR algorithm. Last, the predicted components are added to predict the RUL of the battery. This method solved the problem of low accuracy of individual models and the inability to fully predict the battery degradation trend.
- (2) An improved variational modal decomposition algorithm is proposed. The value of modal layers  $K$  and the penalty parameter  $\alpha$  in the VMD algorithm are generated by the WOA with the minimum envelope entropy as the fitness function. The decomposed components are more easily captured by the subsequent prediction algorithms, which improve the prediction accuracy and are verified in subsequent RUL prediction experiments.

## 2. Prediction Model

### 2.1. Vmd Algorithm

Variational mode decomposition (VMD) is an adaptive signal processing method based on Wiener filtering, which has significant advantages in processing nonlinear and nonstationary signals. Therefore, the VMD model is used to decompose the battery capacity sequence [31]. VMD decomposes the input signal into  $K$  intrinsic mode functions (IMFs), and each mode component  $\mu_k(t)$  surrounds the center frequency  $\omega_k(t)$ . Variational modal decomposition has two steps: constructing and solving variational problems. The construction steps of the variational problem are listed as follows:

Step 1: Solve the unilateral spectrum of each mode component  $\mu_k(t)$  by the Hilbert transform,

$$(\delta(t) + \frac{j}{\pi}) \times \mu_k(t) \quad (1)$$

where  $\delta(t)$  represents the impulse function;

Step 2: Modulate the spectrum of each modal component onto the fundamental band,

$$[(\delta(t) + \frac{j}{\pi}) \times \mu_k(t)] \times e^{-j\omega_k t} \quad (2)$$

Step 3: Construct variational problems according to Formulas (1) and (2),

$$\min_{\{\mu_k\}, \{\omega_k\}} \left\{ \sum_{k=1}^K \left\| \partial_t [(\delta(t) + \frac{j}{\pi}) \times \mu_k(t)] \times e^{-j\omega_k t} \right\|_2^2 \right\} \quad (3)$$

$$\text{s.t. } \sum_{k=1}^K \mu_k(t) = f(t) \quad (4)$$

where  $\partial_t$  represents the partial derivative with respect to  $t$ , and  $K$  is the number of modal components,  $\{\omega_k\} = \{\omega_1, \dots, \omega_K\}$  is the frequency centers of each IMF,  $\{\mu_k\} = \{\mu_1, \dots, \mu_K\}$  represents the  $K$  decomposed IMF components.

To solve the variational problem, introducing the Lagrange operator  $\lambda$  and the quadratic penalty factor  $\alpha$  to Formula (2) turns the constrained conditional variational problem into an unconstrained conditional variational problem:

$$\Gamma(\{\mu_k\}, \{\omega_k\}, \lambda) = \alpha \sum_{k=1}^K \left\| \partial_t \left[ \left( \delta(t) + \frac{j}{\pi} \right) \times \mu_k(t) \right] \times e^{-j\omega_k t} \right\|_2^2 + \left\| f(t) - \sum_{k=1}^K \mu_k(t) \right\|_2^2 - \langle \lambda(t), f(t) - \sum_{k=1}^K \mu_k(t) \rangle. \quad (5)$$

## 2.2. Improvement of the VMD Algorithm

According to the theory of VMD, the number  $K$  of the eigenmode components to be decomposed and the penalty parameter  $\alpha$  will influence the decomposition effect. In VMD, the value of  $K$  determines the number of decomposed IMF components. Excessive  $K$  value will lead to excessive decomposition; otherwise, under-decomposition will occur. The penalty parameter  $\alpha$  determines the bandwidth of the IMF component. The size of the penalty parameter  $\alpha$  is inversely proportional to the bandwidth of the IMF component [32]. The phenomenon of lithium-ion battery capacity rising and falling is complex and changeable. It is vital to select appropriate  $K$  and  $\alpha$  values for the subsequent algorithm to accurately predict the battery life. However,  $K$  and  $\alpha$  are mostly chosen by manual experience, which is likely to influence the decomposition effect of the VMD algorithm.

Entropy is often used to express a signal's degree of randomness and inherent chaos [33]. The smaller the uncertainty of the signal, the stronger the periodicity, and the smaller the entropy value. The more robust the uncertainty of the signal, the greater the interference, and the greater the entropy value. The size of the envelope entropy reflects the sparseness of the signal. The smaller the envelope entropy value is, the stronger the sparseness of the signal and the stronger the periodicity of the decomposed IMF component. In contrast, the signal with a large envelope entropy has weaker sparsity and periodicity. Signals with strong periodicity are more likely to be captured by the LSTM and GPR algorithms, and the information contained in the signal can be better predicted. The whale optimization algorithm (WOA) is a metaheuristic algorithm proposed in 2016 [34]. Simulating the unique bubble net attack hunting behavior of humpback whales is simple to implement, avoids local optimization, and has strong robustness. The WOA has three stages: prey hunting, bubble net predation, and random search. Therefore, in this study, the minimum envelope entropy of the IMF component is employed as the fitness function of the WOA to select the best  $[K, \alpha]$  parameter combination for VMD decomposition. The formula for calculating envelope entropy is expressed as follows:

$$\begin{cases} E_p = - \sum_{i=1}^N p_i \lg p_i \\ p_i = a(i) / \sum_{i=1}^N a_i \end{cases} \quad (6)$$

where the  $p_i$  is the normalized form of  $a(i)$ ,  $a(i)$  is the envelope signal after the signal is demodulated by Hilbert.

The algorithm flow chart of WOA-VMD is shown in Figure 1 and specific steps are described as follows:

- (1) The lithium-ion battery capacity sequence is input, the parameter ranges of  $K$  and  $\alpha$  are set in VMD, and the main parameters in the WOA, including the size of the population, maximum number of iterations, and number of variables, are initialized.
- (2) VMD decomposition is performed on the input capacity sequence, where the number of modal component  $K$  and penalty factor  $\alpha$  are optimized by the WOA, the enve-

lope entropy corresponding to each whale individual is calculated, and the optimal individual position is recorded.

- (3) The location of individual whales is updated.
- (4) Repeat steps (2) to (4) and output the best parameter combination ( $K, \alpha$ ) when the minimum envelope entropy value or the maximum number of iterations is reached;
- (5) VMD decomposition is performed on the signal according to the output parameter combination ( $K, \alpha$ ).

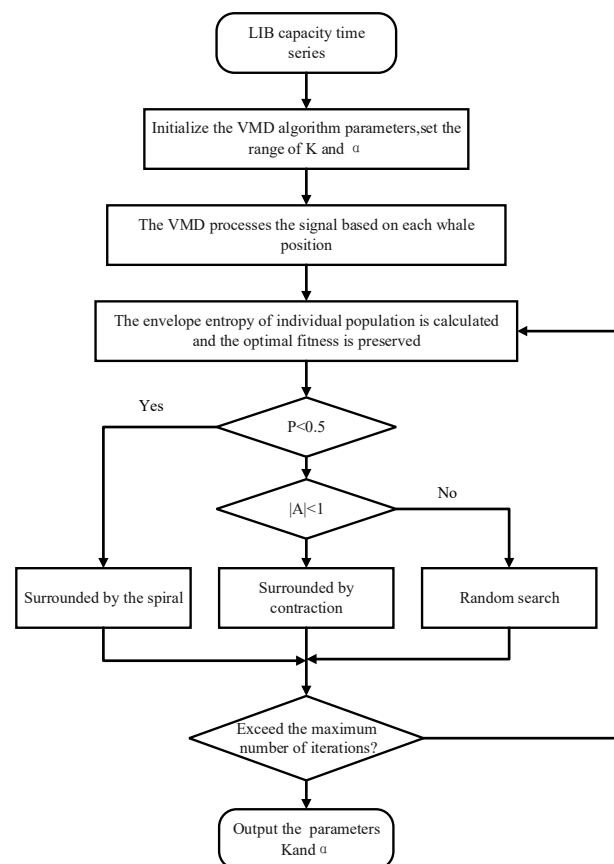


**Figure 1.** Flowchart of the WOA-VMD method.

### 2.3. Experimental Procedures

Aimed at the steep rise and fall of battery capacity, a new integrated method of the RUL prediction of lithium-ion batteries is proposed in this paper. The flow chart of battery RUL prediction is shown in Figure 2, and specific steps are listed as follows:

- (1) Obtain the measured lithium-ion battery capacity degradation data.
- (2) Based on the improved VMD algorithm, the optimal parameter combination [ $K, \alpha$ ] is selected. The lithium-ion battery capacity degradation sequence is decomposed into residual and capacity recovery components through WOA-VMD.
- (3) The residual component obtained after decomposition is trained and predicted by the LSTM network. The residual component reflects the overall degradation trend of the battery and has stability. The LSTM algorithm has a good effect on time series prediction. The decomposed capacity recovery component reflects the capacity regeneration phenomenon of the battery, so the GPR algorithm is selected for fitting prediction.
- (4) The predicted residual component and capacity recovery components are added according to Formula (7) to obtain the predicted capacity data and to simultaneously calculate the RUL of the battery.

$$\hat{y}_i = \sum_{j=1}^n IMF_j + r_s \quad (7)$$

where  $r_s$  is the predicted value of the residual component,  $n$  is the number of decomposed components,  $IMF_j$  is the predicted value of the  $j$ -th capacity escalation component, and  $\hat{y}_i$  is the predicted value of the battery capacity.

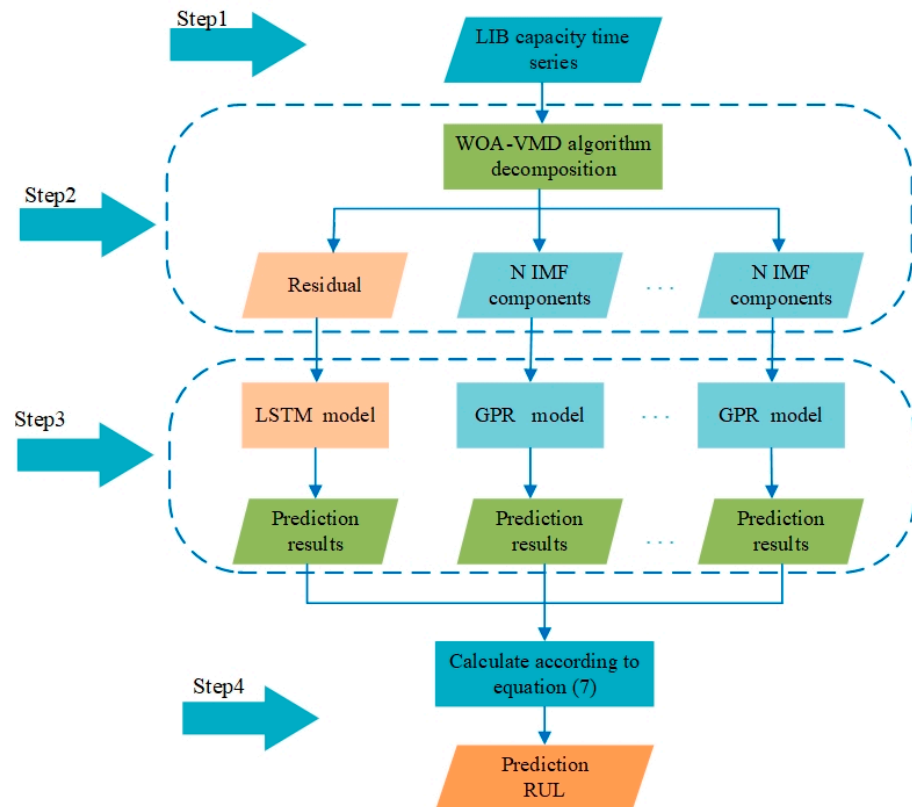


**Figure 2.** Prediction procedure of battery RUL.

### 3. Experimental Verification and Analysis

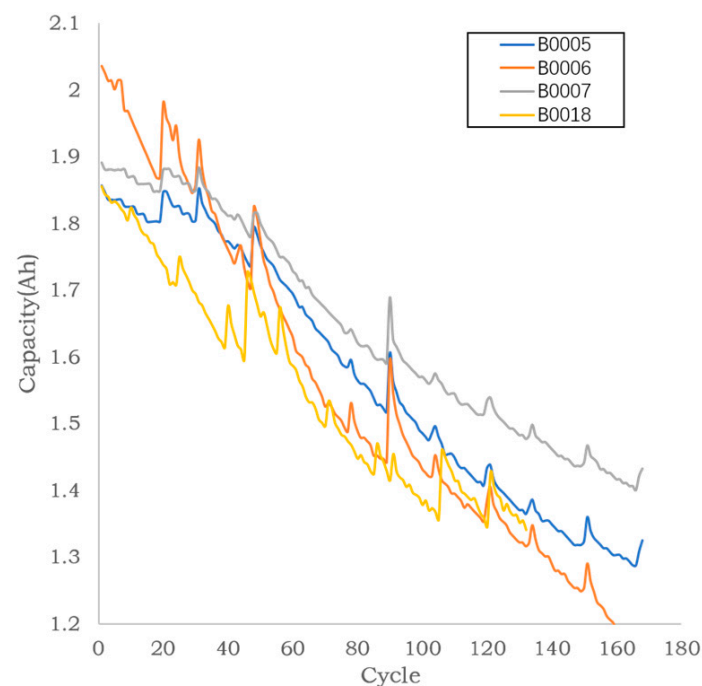
#### 3.1. Datasets

The lithium-ion battery data used in this experiment are from the publicly available dataset of the NASA PCoE Research Center [35,36]. In this study, the first degradation datasets (battery packs B0005, B0006, B0007, and B0018) were selected for experiments to verify the accuracy of the improved VMD-LSTM-GPR for battery RUL prediction. The battery's rated capacity was 2 Ah, and the ambient temperature is set to room temperature (24 °C). The maximum cutoff voltage of the battery while charging is set to 4.2 V. The battery is charged at a constant current of 1.5 A until the battery reaches the maximum cutoff voltage, then the constant voltage charge is maintained until the battery drops to 20 mA. It discharges at a constant current of 2A until the voltage drops to the cutoff value. The parameters of the charge cutoff voltage (CV), discharge current (DC), discharge cutoff voltage (DV), constant current charging current (CC), and battery failure threshold (TS) are shown in Table 1. The discharge curves of the batteries are shown in Figure 3. The battery capacity data have an obvious downward trend and many capacity regeneration phenomena.



**Table 1.** Battery parameters in aging experiment.

Battery Number	CV/V	DV/V	CC/A	DC/A	TS/AH
B0005	4.2	2.7	1.5	2.0	1.4
B0006	4.2	2.5	1.5	2.0	1.4
B0007	4.2	2.2	1.5	2.0	1.4
B0018	4.2	2.5	1.5	2.0	1.4

**Figure 3.** Capacity change curve of NASA PCoE data.

### 3.2. Evaluation Criterion

The RUL of a battery is defined as the number of cycles remaining usable from the predicted starting point to the end of the battery life. This paper selects the mean absolute error (MAE), root mean square error (RMSE), absolute error (AE), and relative error (RE) as the evaluation criteria of the prediction model. The smaller the value of the above evaluation index, the smaller the prediction error and the more accurate the prediction results. The calculation formulas of the four indicators are expressed as follows:

$$MAE = \frac{1}{n} \sum_{i=1}^n |\hat{y}_i - y_i| \quad (8)$$

$$RMSE = \sqrt{\frac{1}{n} \sum_{i=1}^n (\hat{y}_i - y_i)^2} \quad (9)$$

$$AE = |T_{RUL} - \hat{T}_{RUL}| \quad (10)$$

$$RE = \frac{|T_{RUL} - \hat{T}_{RUL}|}{T_{RUL}} \times 100\% \quad (11)$$

where  $n$  is the predicted number of cycles,  $\hat{y}_i$  is the predicted battery capacity value,  $y_i$  is the true capacity value,  $T_{RUL}$  is the true value of the battery RUL, and  $\hat{T}_{RUL}$  is the predicted value of the battery RUL.

### 3.3. Decomposition of Lithium-Ion Battery Capacity Sequence by WOA-VMD

Using the WOA to optimize the VMD parameters ( $K$ ,  $\alpha$ ) can avoid the loss of information or the unsatisfactory decomposition effect caused by the selection of the VMD parameters by manual experience. The subsequent algorithms can also more accurately predict the components obtained by decomposition. The population size of WOA-VMD is set to 10, the maximum number of iterations is set to 30, the iteration range of  $K$  is (4, 6), and the iteration range of  $\alpha$  is (20, 1000). The parameters ( $K$ ,  $\alpha$ ) and minimum envelope entropy of batteries B0005, B0006, B0007, and B0018 decomposed by WOA-VMD are shown in Table 2. The results of the decomposition of the B0005 battery by the WOA-VMD method are shown in Figure 4. IMF1, as a residual component, can show the global degradation tendency of lithium-ion battery capacity performance. Other recovery components can reflect the rapid rise and fall of battery capacity and random fluctuations. After the four battery packs are decomposed by WOA-VMD, the correlation coefficient between the decomposition results and the real capacity data is shown in Table 3. It shows that the capacity recovery component also contains the effective information of the real capacity sequence.

**Table 2.** Results of the optimization of VMD parameters by the WOA.

Battery Number	$K$	$\alpha$	Envelope Entropy
B0005	4	92	6.7876
B0006	4	20	6.837
B0007	4	151	6.7489
B0018	5	709	6.5357

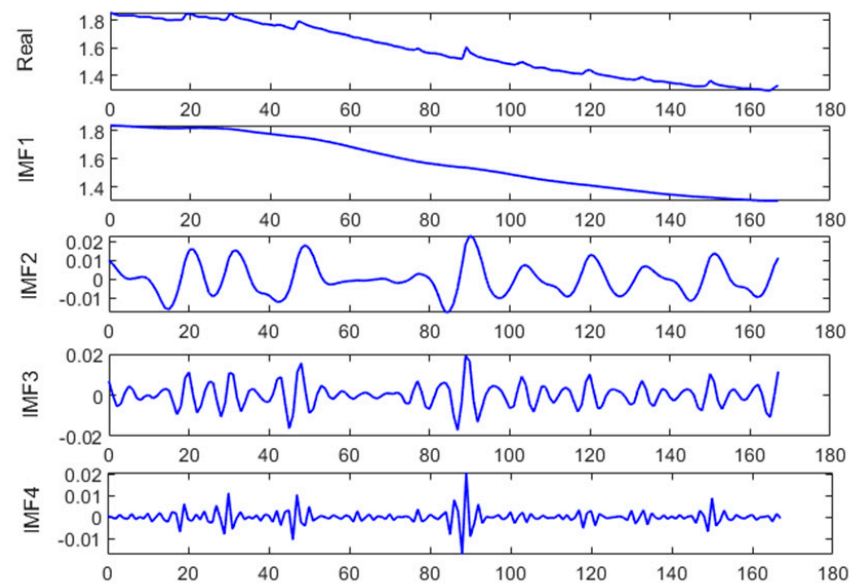


**Figure 4.** WOA-VMD results of B0005 battery capacity data.

**Table 3.** Correlation coefficient between IMFS and measured capacity data for each battery group.

Battery Number	Correlation Coefficient				
	IMF1	IMF2	IMF3	IMF4	IMF5
B0005	0.9979	0.1025	0.0516	0.0325	-
B0006	0.9954	0.1417	0.0669	0.0419	-
B0007	0.9976	0.1142	0.0535	0.0353	-
B0018	0.9931	0.0922	0.0854	0.0507	0.0467



### 3.4. RUL Prediction of LIBs

The lithium-ion battery capacity sequence is decomposed by the improved VMD algorithm, the LSTM is used to train and predict the residual component, and the Gaussian process regression fits the capacity recovery component. Using the B0005 battery as an example, the data of the first 80 residual components are selected as the training set, and the last 88 sets are utilized as the testing set. The capacity data of the first three consecutive times are used to predict the capacity data of the next time, so the number of input nodes is three, and the number of output nodes is 1. Adam is selected as the optimizer of LSTM training, with an initial learning rate of 0.01. After 260 times of training, the model accuracy will no longer rise and remain stable. The specific structure and parameters of LSTM are shown in Table 4. The prediction results of the residual components are shown in Figure 5. The prediction effect and accuracy in the entire testing set are excellent.

**Table 4.** Parameters and structure of LSTM.

Model	Parameters	Values
LSTM	input nodes	3
	output nodes	1
	optimizer	Adam
	learning-rate	0.01
	batchsize	40
	iterations	260

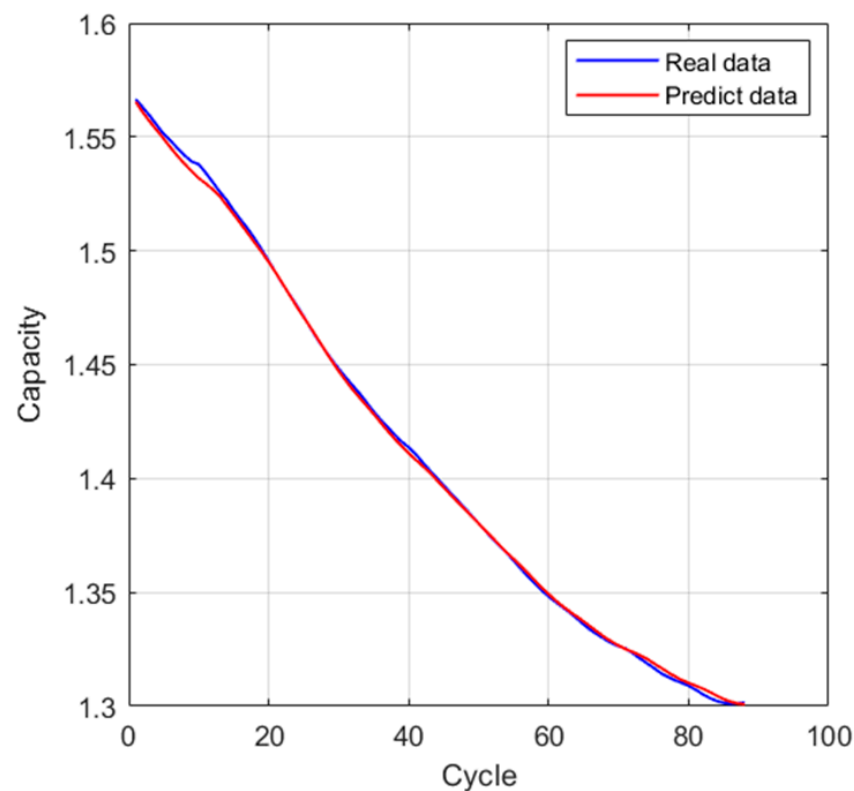


**Figure 5.** Prediction results of residual components of B0005 battery.

With the same training and testing set divisions as the previously described residual components, the three capacity recovery components of the WOA-VMD decomposition are fed to the GPR model for prediction. The predicted results of the recovery components are shown in Figure 6. The GPR model can well capture the fluctuation of the capacity recovery components.

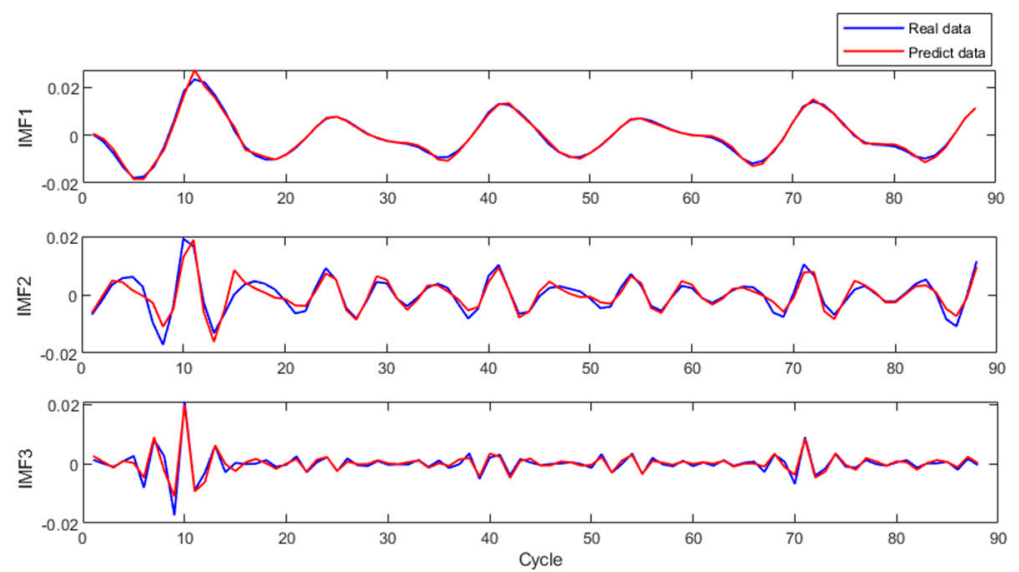


**Figure 6.** Prediction results of the B0005 battery capacity recovery components.

The residual component predicted by LSTM and the capacity recovery components predicted by the GPR model are added according to Formula (7) to obtain the predicted lithium-ion battery capacity. As shown in Figure 7, the predicted battery capacity curve is very close to the actual battery capacity curve. The battery capacity recovery and random fluctuation phenomena are well captured, indicating that the improved VMD-LSTM-GPR method can achieve accurate prediction of the RUL of lithium-ion batteries.

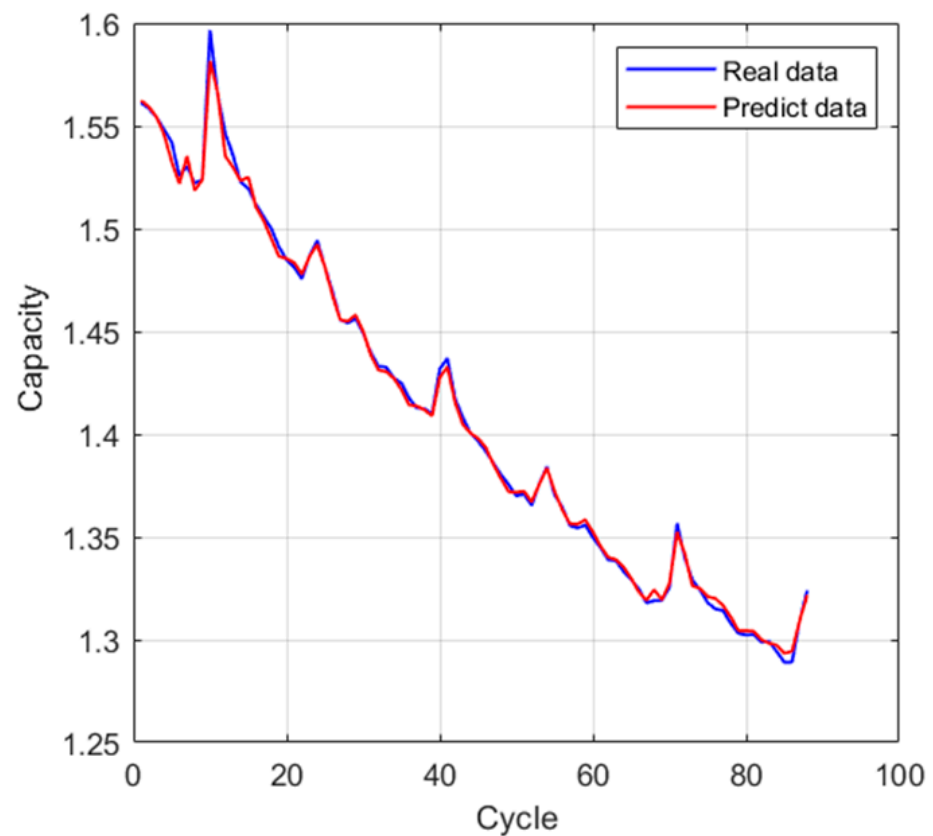


**Figure 7.** Capacity prediction results of the B0005 battery.

To demonstrate the accuracy and robustness of the improved VMD-LSTM-GPR method, separate LSTM, separate GPR, separate EMD-LSTM-GPR, separate VMD-LSTM and VMD-LSTM-GPR were compared with the method proposed in this paper on battery packs of B0005, B0006, B0007 and B0018. In the VMD-LSTM and VMD-LSTM-GPR algorithms,  $K$  of the eigenmode number of the VMD decomposition is directly set manually based on the accumulation of historical experience. The experiments were conducted based on MATLAB 2021a. The B0005, B0006, and B0007 batteries use the first 80 data as the training set. Since the B0018 battery has only 132 data points, B18 uses the first 65 data as the training set. The MAE and RMSE of the five different prediction methods are shown in Table 5.

**Table 5.** Comparison of errors between the algorithm in this paper and the other five methods.

Battery Number	Evaluation Criteria	Propose	LSTM	GPR	EMD-LSTM-GPR	VMD-LSTM	VMD-LSTM-GPR
B0005	MAE	0.0020	0.063	0.083	0.0093	0.0089	0.0023
	RMSE	0.0027	0.085	0.146	0.0136	0.0122	0.0031
B0006	MAE	0.0054	0.092	0.091	0.0097	0.013	0.0071
	RMSE	0.0081	0.113	0.105	0.0146	0.025	0.0086
B0007	MAE	0.0021	0.055	0.073	0.0074	0.0051	0.0024
	RMSE	0.0031	0.063	0.095	0.0112	0.0062	0.0037
B0018	MAE	0.0028	0.039	0.062	0.0085	0.0073	0.0043
	RMSE	0.0040	0.046	0.085	0.0108	0.0092	0.0057

The evaluation indicators in Table 5 show that the integrated method has the highest prediction accuracy and that the prediction error of a single algorithm is relatively large. Among the single models, the LSTM prediction model has the best accuracy, which indicates that the LSTM algorithm has advantages in battery capacity prediction and can predict the capacity degradation trend of the battery pack, so the LSTM algorithm is selected to predict the residual component. Similarly, the GPR algorithm can effectively track the sudden change in capacity degradation, so the GPR algorithm is used to predict the capacity recovery components. Comparing the EMD-LSTM-GPR algorithm with the VMD-LSTM-GPR algorithm, it can be seen that the VMD algorithm can reduce the impact of steep rise and complex drop of capacity sequence on the prediction results more than the EMD algorithm, and it can also reduce the noise of data. A comparison of the method in this paper with the VMD-LSTM-GPR algorithm reveals that the prediction effect of the VMD parameters  $[K, \alpha]$  selected by the WOA is more accurate than the parameters chosen by experience, which shows that the improved VMD algorithm can further reduce the noise interference and improve the prediction accuracy of the algorithm.

### 3.5. Battery RUL Prediction and Comparison with Different Prediction Starting Points

In order to test the robustness and adaptability of the improved VMD-LSTM-GPR method, this paper selects battery data of different training samples for comparative experiments. NASA set the failure threshold of this battery pack to 70% of the standard capacity, so the failure threshold of the battery is 1.4 Ah. Since the capacity data of the B0007 battery are all above 70% of the rated capacity, the other three batteries were chosen for the experiment. The B0005 battery and B0006 battery select the first 80 samples and 100 samples, respectively, as the training set, and the B0018 battery only has 135 pieces of data, so 60 samples and 80 samples are selected as the training set. The prediction results of B0005, the prediction starting points according to the improved VMD-LSTM-GPR method, are shown in Figures 8 and 9.

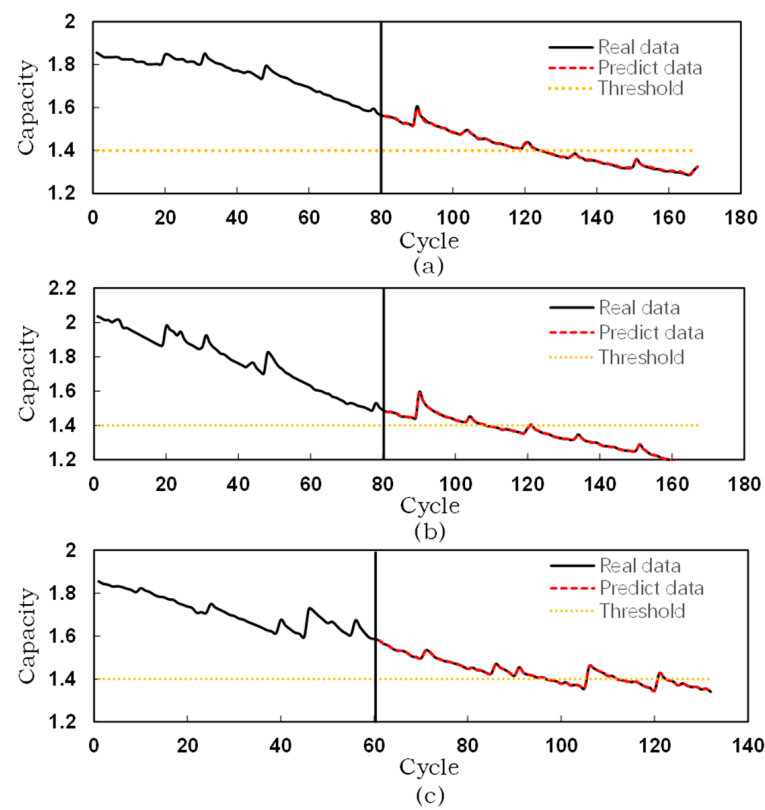


**Figure 8.** Prediction results for B0005 and B0006 with 80 training samples and B0018 with 60 training samples. (a) B0005, (b) B0006, and (c) B0018.

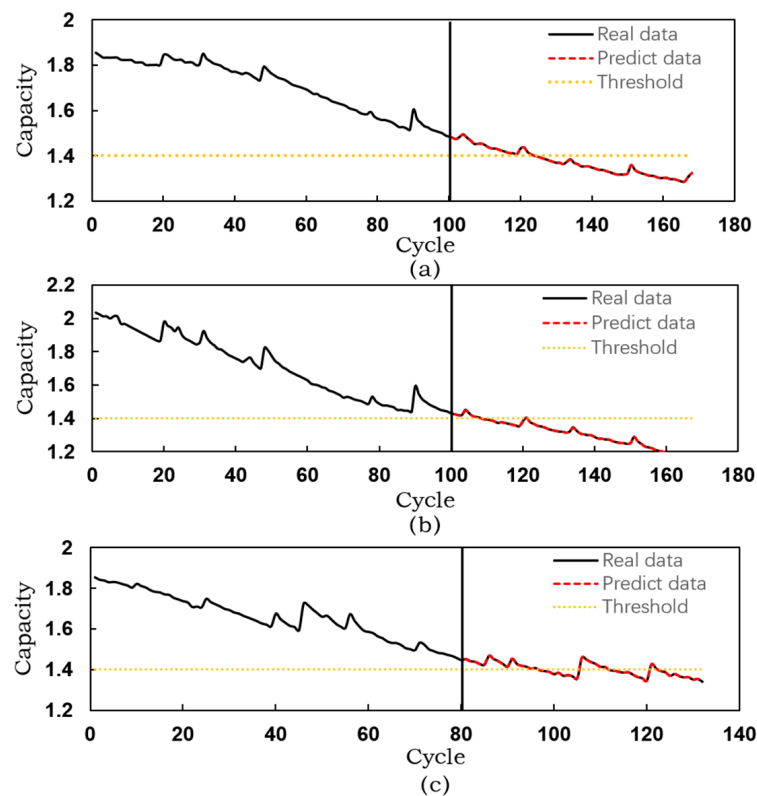


**Figure 9.** Prediction results for B0005 and B0006 with 100. training samples and B0018 with 80 training samples. (a) B0005, (b) B0006, and (c) B0018.

To certify the reliability of the improved VMD-LSTM-GPR method, it is compared with the latest algorithms. Yang et al. [37] proposed an ensemble algorithm based on ensemble empirical pattern decomposition gray wolf optimization support vector regression (EEMD-GWO-SVR) to predict the RUL of batteries. Hu et al. [38] proposed a lithium-ion battery RUL prediction method based on the combination of the PF and LSTM algorithms. Catelani et al. [19] proposed a method based on an RNN to predict the RUL of lithium batteries. Table 6 compares the prediction results of the above three algorithms and the proposed hybrid method.

**Table 6.** Comparison between the algorithm in this paper and other RUL prediction algorithms.

Battery Number	Method	Start	Real	Predict	AE	RE
B0005	EEMD-GWO-SVR	80	44	46	2	4.5
		100	24	26	2	8.3
	PF-LSTM	80	44	41	3	6.8
		100	24	22	2	8.3
	RNN	80	44	50	6	13.6
		100	24	28	4	16.7
	Propose	80	44	44	0	0
		100	24	24	0	0
	EEMD-GWO-SVR	80	28	30	2	7.1
		100	8	10	2	25
	PF-LSTM	80	28	30	2	7.1
		100	8	10	2	25
B0006	EEMD-GWO-SVR	80	28	30	2	7.1
		100	8	10	2	25
	PF-LSTM	80	28	30	2	7.1
		100	8	10	2	25
	RNN	80	28	33	5	17.9
		100	8	7	1	13
	Propose	80	28	29	1	3.6
		100	8	8	0	0
	EEMD-GWO-SVR	60	37	-	-	-
		80	17	17	17	0
	PF-LSTM	60	37	41	4	10.8
		80	17	18	1	5.9
B0018	EEMD-GWO-SVR	60	37	-	-	-
		80	17	16	1	5.9
	PF-LSTM	60	37	-	-	-
		80	17	16	1	5.9
	RNN	60	37	-	-	-
		80	17	16	1	5.9
	Propose	60	37	36	1	2.8
		80	17	18	1	5.9

Table 6 shows that the proposed algorithm has good competitiveness compared with the three compared algorithms (data not provided in the reference are represented by “-”). The AE of each group of batteries does not exceed 1 at different training samples, and the AE of the B0005 battery is 0 at both prediction starting points, which shows that the algorithm of this paper can achieve a high level of prediction without a large number of training samples. The overall RUL prediction results of the three groups of batteries show that the proposed algorithm is generally better than the three compared algorithms. This finding shows that the improved VMD-LSTM-GPR-based method is effective in capturing the capacity recovery phenomenon of lithium-ion batteries and can make an accurate prediction of the battery RUL.

#### 4. Conclusions

In this paper, an improved integrated method of VMD, LSTM, and GPR for the RUL prediction of lithium batteries is proposed for the first time. The improved VMD algorithm decomposes the measured lithium-ion battery capacity degradation sequence to obtain the residual component and capacity recovery components, which can significantly reduce the battery prediction error caused by the capacity random fluctuation phenomenon. The residual component reflects the global degradation trend of the battery capacity. The capacity rising component represents the phenomenon of steep rise and fall of the battery capacity and the random noise during use, where the parameters of VMD  $[K, \alpha]$  are

optimally selected by the WOA, which can avoid the uncertainty arising from the selection of parameters according to manual experience. The LSTM model is used to predict the residual component, and the capacity recovery components are predicted by the GPR model, which solves the low accuracy problem of battery RUL prediction by a single model. The improved VMD-LSTM-GPR method is verified on NASA datasets. The prediction results of B0005, B0006, B0007, and B0018 batteries show that the MAE and RMSE error of the method proposed in this study do not exceed 0.5% and 0.8% respectively, and the absolute error of the RUL prediction does not exceed one cycle. Experiments on the above four battery packs show that the algorithm has better predictive performance compared with a single model, other hybrid models, and the latest literature on battery RUL prediction.

The prediction method proposed in this study uses NASA's dataset, in which the charging and discharging process of the battery has clear restrictions. However, in the actual use scenario of lithium-ion batteries, the working state of the battery will have great randomness. Therefore, we can make efforts in the following aspects in the future. (1) Lithium-ion batteries in general use scenarios are taken as the object of study. (2) Consider adding other features as inputs to the prediction model. (3) Different datasets are chosen to validate the algorithm proposed in this study.

**Author Contributions:** Conceptualization, C.S.; methodology, C.S.; validation, A.Q.; writing—original draft preparation, C.S.; writing—review and editing, C.S.; visualization, Z.J.; supervision, Z.J., J.Z. and Q.S. All authors have read and agreed to the published version of the manuscript.

**Funding:** This work was supported by China Mobile Communications Group Xinjiang Co., Ltd. Development Fund Project under CMXJ-202100687.

**Data Availability Statement:** The lithium-ion battery data used in this experiment are from the publicly available dataset of the NASA PCoE Research Center.

**Conflicts of Interest:** The authors declare no conflict of interest.

## References

- Swornowski, P.J. Destruction mechanism of the internal structure in Lithium-ion batteries used in aviation industry. *Energy* **2017**, *122*, 779–786. [\[CrossRef\]](#)
- Pang, X.; Huang, R.; Wen, J.; Shi, Y.; Jia, J.; Zeng, J. A Lithium-ion Battery RUL Prediction Method Considering the Capacity Regeneration Phenomenon. *Energies* **2019**, *12*, 2247. [\[CrossRef\]](#)
- Wang, F.-K.; Mamo, T. A hybrid model based on support vector regression and differential evolution for remaining useful lifetime prediction of lithium-ion batteries. *J. Power Sources* **2018**, *401*, 49–54. [\[CrossRef\]](#)
- Yun, Z.; Qin, W.; Shi, W.; Ping, P. State-of-Health Prediction for Lithium-Ion Batteries Based on a Novel Hybrid Approach. *Energies* **2020**, *13*, 4858. [\[CrossRef\]](#)
- Khan, H.; Nizami, I.F.; Qaisar, S.M.; Waqar, A.; Krichen, M.; Almaktoom, A.T. Analyzing Optimal Battery Sizing in Microgrids Based on the Feature Selection and Machine Learning Approaches. *Energies* **2022**, *15*, 7865. [\[CrossRef\]](#)
- Tian, H.; Qin, P.; Li, K.; Zhao, Z. A review of the state of health for lithium-ion batteries: Research status and suggestions. *J. Clean. Prod.* **2020**, *261*, 120813. [\[CrossRef\]](#)
- Shimamoto, A.T.; Tanaka, B.R.; Tanaka, C.K. A study on evaluation method for the Lithium-ion battery life performance for stationary use. In Proceedings of the 2013 International Conference on Clean Electrical Power (ICCEP), Alghero, Italy, 11–13 June 2013; pp. 115–119. [\[CrossRef\]](#)
- He, W.; Williard, N.; Osterman, M.; Pecht, M. Prognostics of lithium-ion batteries based on Dempster-Shafer theory and the Bayesian Monte Carlo method. *J. Power Sources* **2011**, *196*, 10314–10321. [\[CrossRef\]](#)
- Zhang, L.; Mu, Z.; Sun, C. Remaining Useful Life Prediction for Lithium-Ion Batteries Based on Exponential Model and Particle Filter. *IEEE Access* **2018**, *6*, 17729–17740. [\[CrossRef\]](#)
- He, Z.; Gao, M.; Xu, J. EKF-Ah Based State of Charge Online Estimation for Lithium-ion Power Battery. In Proceedings of the 2009 International Conference on Computational Intelligence and Security, Beijing, China, 11–14 December 2009; pp. 142–145.
- Xiong, R.; Zhang, Y.; He, H.; Zhou, X.; Pecht, M.G. A Double-Scale, Particle-Filtering, Energy State Prediction Algorithm for Lithium-Ion Batteries. *IEEE Trans. Ind. Electron.* **2017**, *65*, 1526–1538. [\[CrossRef\]](#)
- Kim, S.; Park, H.J.; Choi, J.-H.; Kwon, D. A Novel Prognostics Approach Using Shifting Kernel Particle Filter of Li-Ion Batteries Under State Changes. *IEEE Trans. Ind. Electron.* **2020**, *68*, 3485–3493. [\[CrossRef\]](#)
- Xu, J.; Zhen, A.; Cai, Z.; Wang, P.; Gao, K.; Jiang, D. State of Health Diagnosis and Remaining Useful Life Prediction of Lithium-Ion Batteries Based on Multi-Feature Data and Mechanism Fusion. *IEEE Access* **2021**, *9*, 85431–85441. [\[CrossRef\]](#)



14. Qiu, X.; Wu, W.; Wang, S. Remaining useful life prediction of lithium-ion battery based on improved cuckoo search particle filter and a novel state of charge estimation method. *J. Power Sources* **2020**, *450*, 227700. [\[CrossRef\]](#)
15. Xiong, W.; Mo, Y.; Yan, C. Online State-of-Health Estimation for Second-Use Lithium-Ion Batteries Based on Weighted Least Squares Support Vector Machine. *IEEE Access* **2020**, *9*, 1870–1881. [\[CrossRef\]](#)
16. Zhang, S.; Zhai, B.; Guo, X.; Wang, K.; Peng, N.; Zhang, X. Synchronous estimation of state of health and remaining useful lifetime for lithium-ion battery using the incremental capacity and artificial neural networks. *J. Energy Storage* **2019**, *26*, 100951. [\[CrossRef\]](#)
17. Feng, H.; Song, D. A health indicator extraction based on surface temperature for lithium-ion batteries remaining useful life prediction. *J. Energy Storage* **2020**, *34*, 102118. [\[CrossRef\]](#)
18. Chang, Y.; Fang, H. A hybrid prognostic method for system degradation based on particle filter and relevance vector machine. *Reliab. Eng. Syst. Saf.* **2019**, *186*, 51–63. [\[CrossRef\]](#)
19. Catelani, M.; Ciani, L.; Fantacci, R.; Patrizi, G.; Picano, B. Remaining useful life estimation for prognostics of lithium-ion batteries based on recurrent neural network. *IEEE Trans. Instrum. Meas.* **2021**, *70*, 1–11. [\[CrossRef\]](#)
20. Yang, Y. A machine-learning prediction method of lithium-ion battery life based on charge process for different applications. *Appl. Energy* **2021**, *292*, 116897. [\[CrossRef\]](#)
21. Wei, M.; Gu, H.; Ye, M.; Wang, Q.; Xu, X.; Wu, C. Remaining useful life prediction of lithium-ion batteries based on Monte Carlo Dropout and gated recurrent unit. *Energy Rep.* **2021**, *7*, 2862–2871. [\[CrossRef\]](#)
22. Zhu, T.; Li, Y.; Li, Z.; Guo, Y.; Ni, C. Inter-Hour Forecast of Solar Radiation Based on Long Short-Term Memory with Attention Mechanism and Genetic Algorithm. *Energies* **2022**, *15*, 1062. [\[CrossRef\]](#)
23. Zhang, M.; Kang, G.; Wu, L.; Guan, Y. A method for capacity prediction of lithium-ion batteries under small sample conditions. *Energy* **2022**, *238*, 122094. [\[CrossRef\]](#)
24. Li, X.; Wang, Z.; Yan, J. Prognostic health condition for lithium battery using the partial incremental capacity and Gaussian process regression. *J. Power Sources* **2019**, *421*, 56–67. [\[CrossRef\]](#)
25. Richardson, R.R.; Osborne, M.A.; Howey, D.A. Gaussian process regression for forecasting battery state of health. *J. Power Sources* **2017**, *357*, 209–219. [\[CrossRef\]](#)
26. Yu, J. State of health prediction of lithium-ion batteries: Multiscale logic regression and Gaussian process regression ensemble. *Reliab. Eng. Syst. Saf.* **2018**, *174*, 82–95. [\[CrossRef\]](#)
27. Tong, Z.; Miao, J.; Tong, S.; Lu, Y. Early prediction of remaining useful life for Lithium-ion batteries based on a hybrid machine learning method. *J. Clean. Prod.* **2021**, *317*, 128265. [\[CrossRef\]](#)
28. Ren, L.; Dong, J.; Wang, X.; Meng, Z.; Zhao, L.; Deen, M.J. A Data-Driven Auto-CNN-LSTM Prediction Model for Lithium-Ion Battery Remaining Useful Life. *IEEE Trans. Ind. Inform.* **2020**, *17*, 3478–3487. [\[CrossRef\]](#)
29. Li, X.; Zhang, L.; Wang, Z.; Dong, P. Remaining useful life prediction for lithium-ion batteries based on a hybrid model combining the long short-term memory and Elman neural networks. *J. Energy Storage* **2019**, *21*, 510–518. [\[CrossRef\]](#)
30. Cheng, G.; Wang, X.; He, Y. Remaining useful life and state of health prediction for lithium batteries based on empirical mode decomposition and a long and short memory neural network. *Energy* **2021**, *232*, 121022. [\[CrossRef\]](#)
31. Gai, J.; Shen, J.; Hu, Y.; Wang, H. An integrated method based on hybrid grey wolf optimizer improved variational mode decomposition and deep neural network for fault diagnosis of rolling bearing. *Measurement* **2020**, *162*, 107901. [\[CrossRef\]](#)
32. Li, C.; Peng, T.; Zhu, Y. A Novel Approach for Acoustic Signal Processing of a Drum Shearer Based on Improved Variational Mode Decomposition and Cluster Analysis. *Sensors* **2020**, *20*, 2949. [\[CrossRef\]](#)
33. Lv, H.; Xu, S.; Liu, Y.; Luo, W. Evaluation and Comparison of Air Pollution Governance Performance: An Empirical Study Based on Jiangxi Province. *Sustainability* **2022**, *14*, 15397. [\[CrossRef\]](#)
34. Yang, G.; Zhang, K.; Cheng, R.; Zhang, Y. A Novel Temperature Error Compensation method for MEMS Gyros Based on WOA-SVR. In Proceedings of the 2021 IEEE International Conference on Computer Science, Artificial Intelligence and Electronic Engineering (CSAIEE), Greenville, SC, USA, 20–22 August 2021; pp. 292–295. [\[CrossRef\]](#)
35. Saha, B.; Goebel, K.; Poll, S.; Christophersen, J. Prognostics Methods for Battery Health Monitoring Using a Bayesian Framework. *IEEE Trans. Instrum. Meas.* **2009**, *58*, 291–296. [\[CrossRef\]](#)
36. Qu, J.; Liu, F.; Ma, Y.; Fan, J. A Neural-Network-Based Method for RUL Prediction and SOH Monitoring of Lithium-Ion Battery. *IEEE Access* **2019**, *7*, 87178–87191. [\[CrossRef\]](#)
37. Yang, Z.; Wang, Y.; Kong, C. Remaining Useful Life Prediction of Lithium-Ion Batteries Based on a Mixture of Ensemble Empirical Mode Decomposition and GWO-SVR Model. *IEEE Trans. Instrum. Meas.* **2021**, *70*, 1–11. [\[CrossRef\]](#)
38. Hu, X.; Yang, X.; Feng, F.; Liu, K.; Lin, X. A Particle Filter and Long Short-Term Memory Fusion Technique for Lithium-Ion Battery Remaining Useful Life Prediction. *J. Dyn. Syst. Meas. Control* **2021**, *143*, 061001. [\[CrossRef\]](#)

**Disclaimer/Publisher’s Note:** The statements, opinions and data contained in all publications are solely those of the individual author(s) and contributor(s) and not of MDPI and/or the editor(s). MDPI and/or the editor(s) disclaim responsibility for any injury to people or property resulting from any ideas, methods, instructions or products referred to in the content.